

## **Full Engineering Laboratory Report**

MAE 108 Aerospace Laboratory

Lab 3 Clark Y-14 Airfoil Drag and Lift

### Group Members:

Kevin Naraki Kim Wong (Group Leader)

Noah Palanjan (Primary Data Collector)

Matthew Valencia (Primary Data Collector)

Triet Ho (Analyst)

Yonghao Huo (Analyst)

Josue Guerrero (Technician)

Devrajsinh Mayurdhvajsinh Zala (Technician)

Vanessa Abigail Renderos

Tristan Reyes

Xuanqi Zang.

### Advisers:

T.A. Cody Gonzalez

Prof. Sherif Hassaan

Date of Experiment: October 31, 2024

Submission Date: November 21, 2024

## Table of Contents

<b>Nomenclature List.....</b>	<b>i</b>
<b>List of Figures.....</b>	<b>ii</b>
<b>List of Tables.....</b>	<b>iii</b>
<b>1. Abstract.....</b>	<b>1</b>
<b>2. Introduction.....</b>	<b>1</b>
<b>3. Background and previous work.....</b>	<b>3</b>
<b>4. Theoretical presentation.....</b>	<b>4</b>
4.1 Lift and Drag Forces.....	4
4.2 Coefficients of Lift, Drag, and Moment.....	5
4.3 Influence of Slats and Flaps.....	5
4.4 Wall Corrections.....	6
4.5 Theoretical Lift Curve Slope.....	6
<b>5. Experimental procedure.....</b>	<b>7</b>
5.1 Calibration.....	7
5.2 Insert airfoil configuration.....	7
5.3 Record data.....	7
<b>6. Results.....</b>	<b>8</b>
<b>7. Conclusion.....</b>	<b>16</b>
<b>8. Acknowledgments .....</b>	<b>16</b>
<b>9. References.....</b>	<b>16</b>
<b>10. Appendices: .....</b>	<b>17</b>
Appendix 1: Sample computations.....	17
Appendix 2: Experimental data.....	20

## Nomenclature List

SYMBOL	DEFINITION
$\alpha$	Angle of attack (degrees)
$c$	Chord length of the airfoil (m)
$C_D$	Drag coefficient (dimensionless)
$C_L$	Lift coefficient (dimensionless)
$C_m$	Pitching moment coefficient (dimensionless)
$D$	Drag force (lbf)
$F_a$	Axial force (N)
$F_n$	Normal force (N)
$L$	Lift force (N)
$M$	Pitching moment about the aerodynamic center ( $Nm$ )
$q$	Dynamic pressure (Pa)
$S$	Reference area ( $m^2$ )
$T_y$	Pitching moment ( $Nm$ )

## List of Figures

<b>Figure 1:</b> Variation of Lift Coefficient ( $C_L$ ) with Angle of Attack ( $\alpha$ ) for the Clark Y-14 Airfoil at Different Free-Stream Velocities (10 m/s, 20 m/s, and 25 m/s). . . . .	8
<b>Figure 2:</b> Drag Coefficient ( $C_D$ ) Variation with Angle of Attack ( $\alpha$ ) for Clark Y-14 Airfoil at Different Free-Stream Velocities (10 m/s, 20 m/s, and 25 m/s) . . . . .	9
<b>Figure 3:</b> Variation of Pitching Moment Coefficient about Aerodynamic Center ( $C_{m,ac}$ ) with Angle of Attack ( $\alpha$ ) for the Clark Y-14 Airfoil at Free-Stream Velocities of 10 m/s, 20 m/s, and 25 m/s. . . . .	10
<b>Figure 4:</b> Lift Coefficient ( $C_L$ ) vs. Angle of Attack ( $\alpha$ ) for Clark Y-14 Airfoil Configurations: Clean, Slat, 45° Flap, and Combined Slat-Flap. . . . .	10
<b>Figure 5:</b> Drag Coefficient ( $C_D$ ) vs. Angle of Attack ( $\alpha$ ) for Various Configurations of the Clark Y-14 Airfoil: Clean, Slat, 45° Flap, and Combined Slat-Flap. . . . .	11
<b>Figure 6:</b> Pitching Moment Coefficient about the Aerodynamic Center ( $C_{m,ac}$ ) vs. Angle of Attack ( $\alpha$ ) for Clark Y-14 Airfoil Configurations: Clean, Slat, 45° Flap, and Combined Slat-Flap. . . . .	12
<b>Figure 7:</b> Comparison of Experimental and Theoretical Lift Coefficient ( $C_L$ ) vs. Angle of Attack ( $\alpha$ ) for the Clark Y-14 Airfoil. . . . .	13
<b>Figure 8:</b> Comparison of Experimental and Theoretical Drag Coefficient ( $C_D$ ) vs. Angle of Attack ( $\alpha$ ) for the Clark Y-14 Airfoil. . . . .	13
<b>Figure 9:</b> Comparison of Experimental and Theoretical Pitching Moment Coefficient ( $C_m$ ) vs. Angle of Attack ( $\alpha$ ) for the Clark Y-14 Airfoil. . . . .	14
<b>Figure 10:</b> Lift Coefficient ( $C_L$ ) vs. Angle of Attack ( $\alpha$ ) for the Clark Y-14 Airfoil with Clean Configuration and Flaps at 30° and 45°. . . . .	14
<b>Figure 11:</b> Drag Coefficient ( $C_D$ ) vs. Angle of Attack ( $\alpha$ ) for the Clark Y-14 Airfoil with Clean Configuration and Flaps at 30° and 45°. . . . .	15
<b>Figure 12:</b> Lift-to-Drag Ratio ( $\frac{L}{D}$ ) vs. Angle of Attack ( $\alpha$ ) for the Clark Y-14 Airfoil with Clean Configuration and Flaps at 30° and 45°. . . . .	15

## List of Tables

<b>Table 1:</b> Clean airfoil with velocity at 0 m/s. ....	20
<b>Table 2:</b> Clean airfoil with velocity at 10 m/s. ....	21
<b>Table 3:</b> Clean airfoil with velocity at 20 m/s. ....	22
<b>Table 4:</b> Clean airfoil with velocity at 25 m/s. ....	23
<b>Table 5:</b> Airfoil with Slat and 5 mm separation, velocity at 0 m/s. ....	24
<b>Table 6:</b> Airfoil with Slat and 5 mm separation, velocity at 20 m/s. ....	25
<b>Table 7:</b> Airfoil with Slat/Flap, 45° Flap, 5 mm separation, and velocity at 0 m/s. ....	26
<b>Table 8:</b> Airfoil with Slat/Flap, 45° Flap, 5 mm separation, and velocity at 20 m/s. ....	27
<b>Table 9:</b> Airfoil with Flap, 45° Flap, and velocity at 0 m/s. ....	28
<b>Table 10:</b> Airfoil with Flap, 45° Flap, and velocity at 20 m/s. ....	29
<b>Table 11:</b> Airfoil with Flap, 30° Flap, and velocity at 0 m/s. ....	30
<b>Table 12:</b> Airfoil with Flap, 30° Flap, and velocity at 20 m/s. ....	31

## **1. Abstract**

The Clark Y-14 airfoil, in clean, slat-only, flap-only, and combined slat-flap configurations, was tested in a wind tunnel to measure the variation in aerodynamic forces across different angles of attack. A force balance measured the lift, drag, and pitching moment, with different flap angles examined to assess aerodynamic behavior. The results showed that slats and flaps significantly improved the lift-to-drag ratio at higher angles of attack, while the clean configuration demonstrated greater efficiency at lower angles. The slat-flap combination provided the greatest lift improvement, emphasizing the role of these control surfaces in enhancing airfoil performance under critical flight conditions.

## **2. Introduction**

In the study of aerodynamics, understanding the behavior of airfoils under various conditions is essential for the development and optimization of aircraft performance. Airfoil characteristics such as lift, drag, and pitching moment coefficients are critical parameters that define the efficiency of a wing or blade. These properties are often influenced by the airfoil's shape and the addition of auxiliary control surfaces such as slats and flaps. The Clark Y-14 airfoil, known for its flat lower surface and moderate camber, is frequently used as a benchmark in aerodynamics research. This airfoil is valued for its simple design and stable performance, making it a useful reference in testing and optimization studies. However, optimizing the lift-to-drag ratio across varying flight conditions requires an in-depth understanding of how airfoil configuration impacts airflow dynamics and the forces acting on the airfoil.

This experiment aims to address this challenge by examining how different configurations of the Clark Y-14 airfoil, specifically the addition of a leading-edge slat and trailing-edge flap, influence its aerodynamic behavior. A core objective is to understand how these control surfaces affect the airflow over the airfoil and how they influence the key aerodynamic forces—lift, drag, and pitching moment—at varying angles of attack. By investigating these configurations, the study aims to enhance understanding of the performance

characteristics of the Clark Y-14 airfoil, particularly in terms of its stall behavior, which is crucial for determining the maximum angle at which it can maintain lift.

To achieve this, a wind tunnel experiment will be conducted, where the lift, drag, and pitching moment of the airfoil will be measured in several configurations: clean, with a slat, with a flap, and with both slat and flap. Additionally, the impact of flap deflection on aerodynamic behavior will be assessed. The experiment will utilize a force balance to quantify the forces and moments acting on the airfoil and will focus on determining the stall characteristics of each configuration. This is particularly important because stall - the rapid loss of lift due to airflow separation - poses a critical limitation in the performance of airfoils.

Understanding how slats and flaps affect the stall characteristics of an airfoil is a central focus of this experiment. Slat, which are mounted on the leading edge of the airfoil, help to delay flow separation by allowing higher-energy air from the lower surface to energize the upper boundary layer, thereby improving lift at higher angles of attack. Flaps, typically mounted on the trailing edge, increase the camber of the airfoil when deployed, which enhances lift production, especially at lower speeds. By analyzing the performance of the Clark Y-14 airfoil in various configurations, this study seeks to provide valuable insights into how these auxiliary devices can improve aerodynamic efficiency and stall resistance.

This experiment is not only important for advancing fundamental aerodynamic research but also holds practical implications for the design and optimization of airfoils in real-world applications. By examining the interaction between airfoil configuration and aerodynamic forces, the results of this study will contribute to a broader understanding of how control surfaces like slats and flaps can be used to enhance the performance and safety of aircraft in different flight regimes. The report is structured as follows: the Background and Previous Work section provides a review of existing research and theoretical concepts relevant to this study. The Theoretical Presentation explains the necessary aerodynamic theory and the associated equations used for analysis. The Experimental Procedure outlines the steps taken to conduct the wind tunnel experiment, followed by the Results section, which presents the data collected from the experiments. The interpretation of Results discusses the implications of the findings, answering specific questions posed by the experiment. Finally, the Conclusions and Acknowledgements

summarize the outcomes of the experiment and provide suggestions for future research and improvements.

### **3. Background and previous work**

The study of the aerodynamic forces acting on an airfoil, particularly lift and drag, is fundamental to optimizing aircraft performance and efficiency. The lift and drag coefficients, along with the pitching moment, are key parameters that characterize an airfoil's ability to generate the necessary forces for flight while minimizing resistance. A significant amount of research has been conducted to understand how different airfoil designs and configurations influence these forces, especially in low-speed and high-lift applications. One of the most widely studied airfoils in this context is the Clark Y-14, which is known for its predictable lift characteristics and stable aerodynamic behavior across a range of speeds and angles of attack. The moderate camber of the Clark Y-14 airfoil makes it a suitable candidate for testing various auxiliary control surfaces like slats and flaps, which are commonly used in modern aircraft to improve performance.

Previous research has shown that the addition of auxiliary devices such as slats and flaps can significantly improve the aerodynamic performance of an airfoil. Slats, mounted on the leading edge of the airfoil, create a gap that allows high-energy air from below the wing to flow over the top surface. This process helps to delay flow separation and extends the operational range of the airfoil by enabling it to sustain higher angles of attack without stalling. Studies from the early 20th century, such as those by Jacobs and Sherman, demonstrated that slats could improve lift performance by as much as 30% at critical angles of attack [2]. The effectiveness of slats in delaying stall has been well-documented, and more recent computational studies using computational fluid dynamics (CFD) have further validated these findings.

Flaps, on the other hand, are mounted on the trailing edge of the airfoil and serve to increase the effective camber when deployed. This results in a higher lift coefficient, particularly at lower speeds. Extensive research on trailing-edge flaps has shown their effectiveness in enhancing lift during takeoff and landing, where additional lift is necessary to compensate for slower airspeeds. Investigations by researchers such as NACA and later by modern CFD



simulations have consistently shown that the deployment of trailing-edge flaps results in significant increases in lift, though it also tends to increase drag. The tradeoff between lift and drag is a central consideration when designing flaps, and their performance depends on the specific configuration and operational conditions.

The relationship between flow separation and stall has also been a major focus of aerodynamic research. Traditional studies, such as those conducted by the NACA, have shown that the lift coefficient increases with the angle of attack up to a critical point, beyond which flow separation occurs and results in a rapid loss of lift. The stall angle, which is the maximum angle at which an airfoil can maintain lift, is crucial in determining the airfoil's performance characteristics. More recent studies, including those using wind tunnel testing and CFD simulations, have provided detailed insights into how flow separation and stall characteristics are influenced by the shape and configuration of the airfoil.

This experiment builds on these foundational studies by focusing on the specific aerodynamic performance of the Clark Y-14 airfoil in different configurations. By examining the effects of slats and flaps on the lift, drag, and pitching moment coefficients at various angles of attack, this research aims to further understand how these modifications impact the stall characteristics and overall aerodynamic efficiency of the airfoil. The findings from this study will contribute to knowledge on airfoil optimization and provide valuable insights for future airfoil design and performance enhancement.

## **4. Theoretical presentation**

The fundamental goal of this experiment is to measure aerodynamic forces in different configurations of the airfoil - clean, with a slat, with a flap, and with both slat and flap - at varying angles of attack, and to analyze how these modifications impact the overall performance of the airfoil.

### **4.1 Lift and Drag Forces**

Lift and drag forces on an airfoil arise due to the pressure distribution and viscous forces acting on its surface as air flows over it. Lift is defined as the component of aerodynamic force acting perpendicular to the free-stream flow direction, while drag is the component acting parallel to the flow direction. These forces depend on factors such as the angle of attack, airfoil

shape, and velocity. In the experiment, the lift (L) and drag (D) forces can be expressed in terms of the normal ( $F_n$ ) and axial ( $F_a$ ) forces, as follows:

$$L = F_n \cos \alpha - F_a \sin \alpha \quad (\text{Equation 4.1.1})$$

$$D = F_a \cos \alpha + F_n \sin \alpha \quad (\text{Equation 4.1.2})$$

where  $\alpha$  is the angle of attack. At zero degrees, the normal force aligns with lift, and the axial force aligns with drag. However, at non-zero angles, both forces must be resolved into lift and drag components.

#### 4.2 Coefficients of Lift, Drag, and Moment

To compare results across different airspeeds and airfoil configurations, the lift, drag, and pitching moment forces are often expressed as non-dimensional coefficients. These coefficients are normalized by dynamic pressure ( $q = \frac{1}{2} \rho V^2$ ) and reference area (S), as shown below:

$$C_L = \frac{L}{q \cdot S} \quad (\text{Equation 4.2.1})$$

$$C_D = \frac{D}{q \cdot S} \quad (\text{Equation 4.2.2})$$

$$C_M = \frac{M}{q \cdot S \cdot c} \quad (\text{Equation 4.2.3})$$

where M is the pitching moment about the aerodynamic center, and c is the chord length of the airfoil. These non-dimensional coefficients are crucial for understanding the aerodynamic efficiency and performance of the airfoil under various configurations.

#### 4.3 Influence of Slats and Flaps

Theoretical studies indicate that the addition of leading-edge slats and trailing-edge flaps alters the pressure distribution around an airfoil, affecting both lift and drag. Slats work by energizing the boundary layer, which helps delay flow separation and maintains lift at higher angles of attack. This is achieved by creating a narrow gap on the leading edge, through which high-energy air from below the wing flows, re-energizing the flow over the upper surface. The

delayed flow separation allows the airfoil to sustain lift at higher angles of attack, which is beneficial for improving maneuverability and delay in stall. Flaps, when deployed on the trailing edge of an airfoil, increase its effective camber, which increases the lift coefficient.

For the clean airfoil, flow separation typically occurs at a lower angle of attack. However, when a slat is added, the separation point moves downstream, allowing the airfoil to maintain lift at higher angles of attack before stalling. Similarly, the addition of a flap increases the lift coefficient, though at the cost of increased drag. The combined effect of both devices on the  $\frac{L}{D}$  ratio is critical, especially for takeoff and landing conditions where high lift is required.

#### 4.4 Wall Corrections

Because the wind tunnel environment is confined, wall interference effects must be considered. These effects, known as wall proximity effects, alter the flow pattern around the airfoil compared to real-world, unconfined conditions. Corrections are therefore applied to account for the influence of the tunnel walls on the angle of attack and drag coefficient. The corrected angle of attack ( $\alpha'$ ) and drag coefficient ( $C_D'$ ) are given by:

$$\alpha' = \alpha + \Delta\alpha \quad (\text{Equation 4.4.1})$$

$$C_D' = C_D + \Delta C_D \quad (\text{Equation 4.4.2})$$

where  $\Delta\alpha$  and  $\Delta C_D$  are correction factors derived from the lift coefficient and the geometry of the test section. These corrections ensure that the wind tunnel data accurately reflects the airfoil's performance in real-world conditions.

#### 4.5 Theoretical Lift Curve Slope

For thin airfoils in incompressible flow, the theoretical lift curve slope ( $\frac{dC_L}{d\alpha}$ ) can be approximated by  $2\pi$  radians, or approximately 0.11 per degree. This theoretical value provides a baseline for comparing experimental data. By comparing the experimental lift curve slope for the clean airfoil with that of the modified configurations (with slats and/or flaps), one can quantify the enhancement in lift performance provided by these modifications.

## **5. Experimental procedure**

The procedure for this experiment involves measuring the lift, drag, and pitching moment coefficients for various configurations of the Clark Y-14 airfoil. The goal is to determine the aerodynamic behavior of each configuration and identify the stall characteristics, which are essential for evaluating the airfoil's performance in different flight conditions.

### **5.1 Calibration**

Before beginning the experiment, it is important to ensure that the measurement equipment is properly calibrated.

1. Run a measurement and verify zero readings on the force balance to ensure it is properly set.
2. Configure a calibration weight (less than 400 g) and place it at one set position on the sting balance.
3. Run a measurement and record the forces and moments. Compare the measured values to the applied values and repeat the procedure with the weight placed at a different location.
4. Repeat the process for two additional weights to verify the accuracy of the measurements.

### **5.2 Insert Airfoil Configuration**

The airfoil configurations to be tested include:

1. Clean airfoil: Test at 10 m/s, 20 m/s, and 25 m/s.
2. Airfoil with slat: Test at 20 m/s with a slat separation of 5 mm.
3. Airfoil with slat and flap: Test at 20 m/s with a slat separation of 5 mm and a flap angle of  $45^\circ$ .
4. Airfoil with flap: Test at 20 m/s with a flap angle of  $45^\circ$ .
5. Flap variation: Test at 20 m/s with a flap angle of  $30^\circ$ .

For each configuration, the experiment will be repeated, and measurements of the normal and axial forces, as well as pitching moments, will be recorded at varying angles of attack.

### **5.3 Record data**

Data should be collected at various angles of attack, with increments specified below:

1. Angle of attack from  $-6^\circ$  to  $30^\circ$  at  $2^\circ$  increments.
2. Angle of attack from  $-4^\circ$  to  $8^\circ$  beyond the stall point at  $4^\circ$  increments.
3. Angle of attack from  $8^\circ$  beyond stall to  $-6^\circ$  at  $4^\circ$  increments.
4. Record the normal, axial force, and pitching moment for each angle.

## 6. Results

$C_L$  vs. Angle of attack

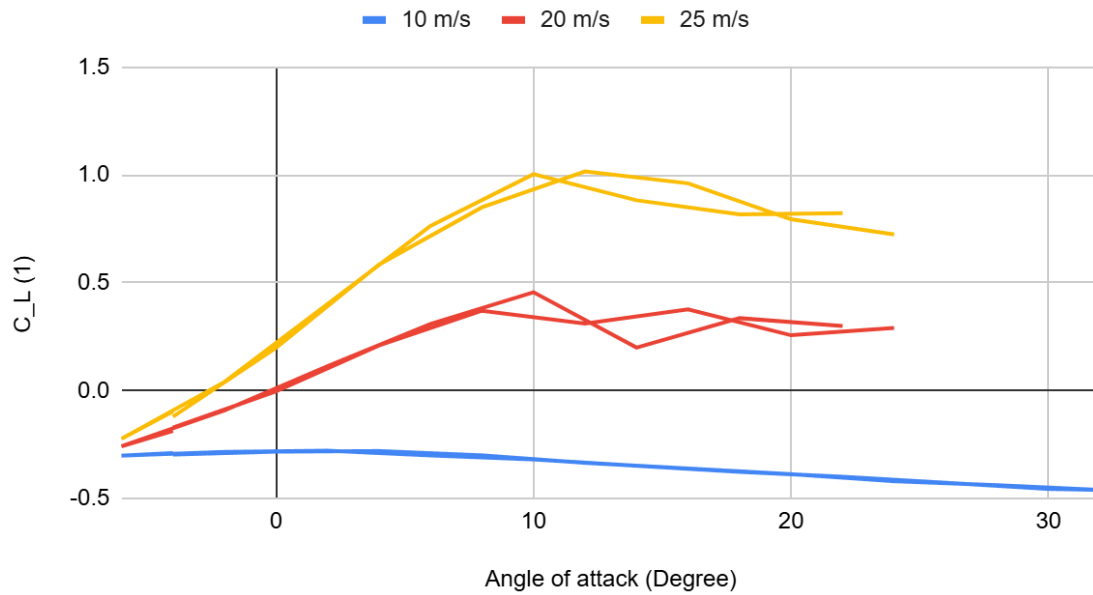
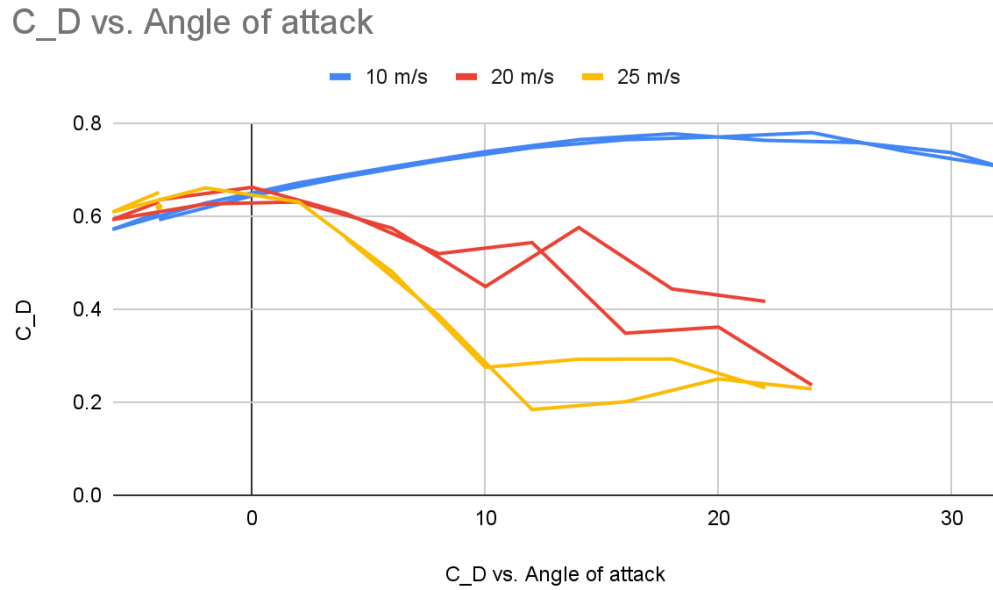


Figure 1: Variation of Lift Coefficient ( $C_L$ ) with Angle of Attack ( $\alpha$ ) for the Clark Y-14 Airfoil at Different Free-Stream Velocities (10 m/s, 20 m/s, and 25 m/s).

The addition of slats and flaps significantly improved the airfoil's performance, particularly at higher angles of attack. For instance, as indicated in Equation 4.1.1 and Equation 4.1.2, the lift ( $L$ ) and drag ( $D$ ) forces are resolved from the normal force ( $F_n$ ) and axial force ( $F_a$ ) measurements, which were shown to be higher for the slat-flap configuration compared to the clean configuration. This was reflected in the lift coefficient ( $C_L$ ), as calculated by Equation 4.2.3, and the drag coefficient ( $C_D$ ) calculated using Equation 4.2.4. At a  $20^\circ$  angle of attack, the combined slat-flap configuration achieved a lift coefficient of approximately 0.25 at 20 m/s,

compared to 0.18 for the clean airfoil as illustrated in Figure 1 ( $C_L$  vs. *Angle of Attack*) and Figure 4 ( $C_L$  vs. *Angle of Attack*). This increase in lift demonstrates the role of slats in delaying flow separation and increasing the effective camber of the airfoil, which is further augmented by the flap. The clean configuration, however, still maintained a more favorable lift-to-drag ratio ( $\frac{L}{D}$ ) at lower angles of attack, highlighting its efficiency at cruising conditions.



*Figure 2: Drag Coefficient ( $C_D$ ) Variation with Angle of Attack ( $\alpha$ ) for Clark Y-14 Airfoil at Different Free-Stream Velocities (10 m/s, 20 m/s, and 25 m/s)*

$C_{m,ac}$  vs. Angle of attack

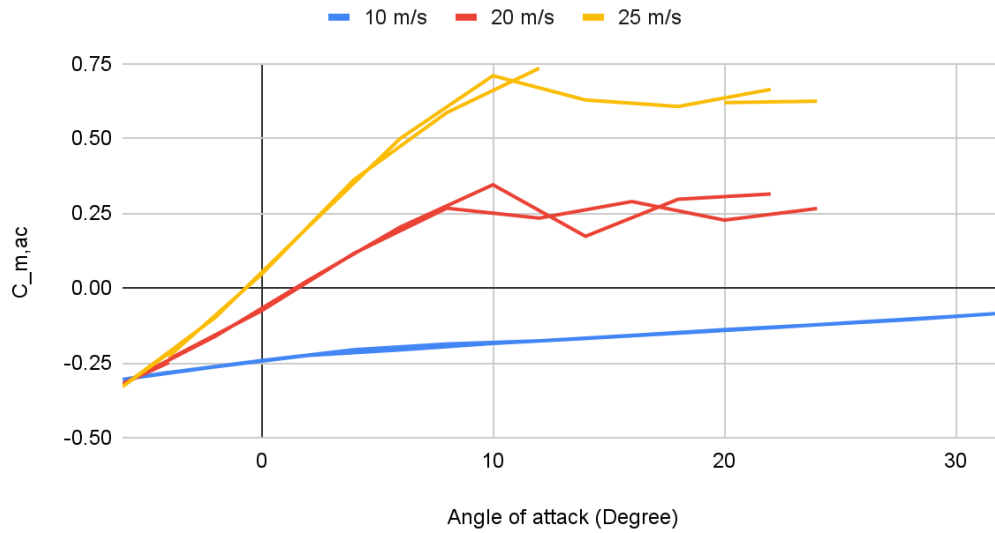


Figure 3: Variation of Pitching Moment Coefficient about Aerodynamic Center ( $C_{m,ac}$ ) with Angle of Attack ( $\alpha$ ) for the Clark Y-14 Airfoil at Free-Stream Velocities of 10 m/s, 20 m/s, and 25 m/s.

$C_L$  vs. Angle of attack

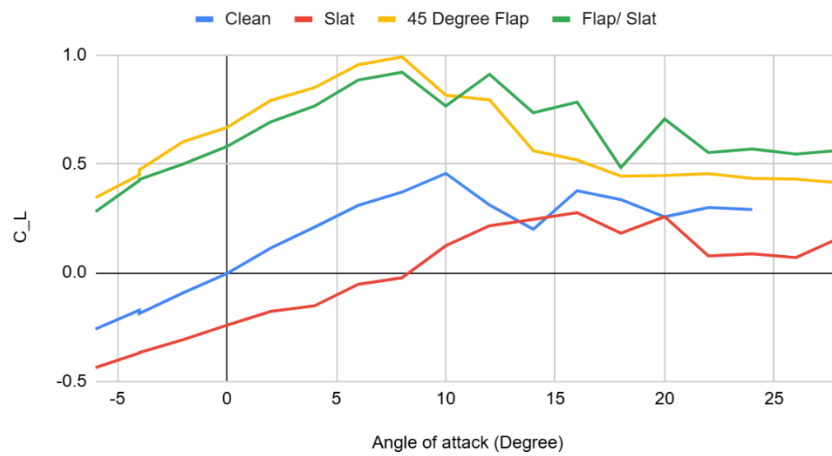


Figure 4: Lift Coefficient ( $C_L$ ) vs. Angle of Attack ( $\alpha$ ) for Clark Y-14 Airfoil Configurations: Clean, Slat, 45° Flap, and Combined Slat-Flap

## C<sub>D</sub> vs. Angle of attack

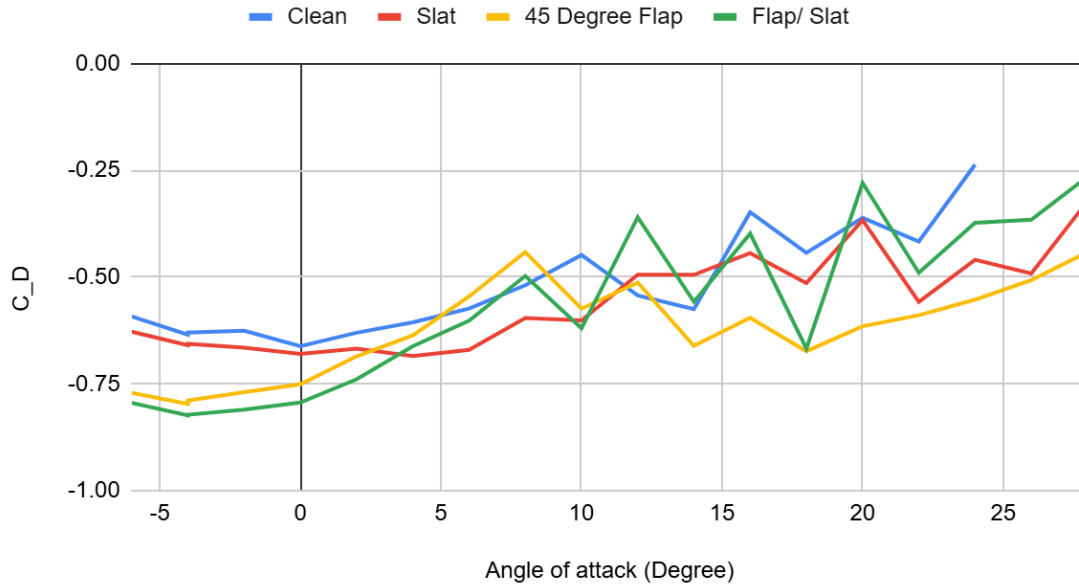


Figure 5: Drag Coefficient ( $C_D$ ) vs. Angle of Attack ( $\alpha$ ) for Various Configurations of the Clark Y-14 Airfoil: Clean, Slat, 45° Flap, and Combined Slat-Flap

Drag coefficient data confirmed these findings. As shown in Figure 2 ( $C_D$  vs. *Angle of Attack*) and Figure 5 ( $C_D$  vs. *Angle of Attack*), the clean configuration maintained lower drag values at lower angles of attack, making it more efficient in cruise conditions. In Equation 4.2.4, the drag coefficient increased for the slat-flap configuration at higher angles of attack, but the increase in drag was accompanied by a larger increase in lift, which ultimately improved the lift-to-drag ratio at critical flight conditions, such as takeoff and landing. This highlights the importance of understanding the tradeoff between lift and drag when designing for different phases of flight. Specifically, the increase in drag with the slat-flap configuration was not as detrimental as it might appear, as the improved lift more than compensated for the added drag, as shown by the higher  $C_L$  values for the combined configuration.



$C_{m,ac}$  vs. Angle of attack

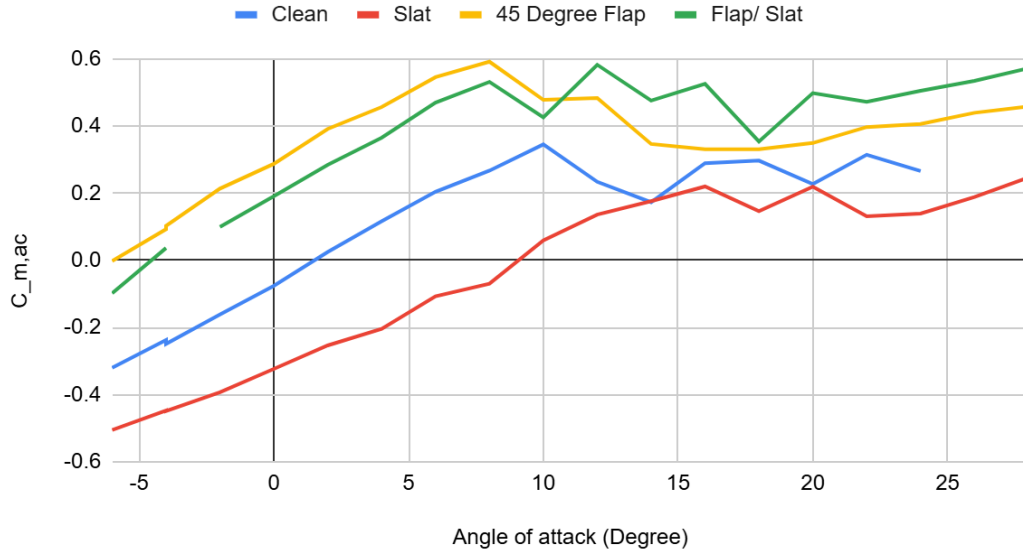


Figure 6: Pitching Moment Coefficient about the Aerodynamic Center ( $C_{m,ac}$ ) vs. Angle of Attack ( $\alpha$ ) for Clark Y-14 Airfoil Configurations: Clean, Slat, 45° Flap, and Combined Slat-Flap

The pitching moment analysis, derived from Equation 4.2.5 and illustrated in Figure 3 ( $C_{M,ac}$  vs. Angle of Attack) and Figure 6 ( $C_{M,ac}$  vs. Angle of Attack), provided further insight into the stability of the airfoil. The pitching moment coefficient ( $C_M$ ) of the clean configuration showed larger fluctuations, indicating that the airfoil was less stable near the stall angle compared to the slat-flap configuration. The combined slat-flap configuration allowed for smoother variations in the pitching moment, indicating better stability and control as the angle of attack increased. The stall angle for the clean configuration was approximately 16°, whereas the addition of the slat and flap delayed stall to around 20°, confirming that these modifications extended the operational range of the airfoil. This result aligns with the theoretical predictions for stall characteristics, where slats help delay flow separation and increase the critical angle of attack.

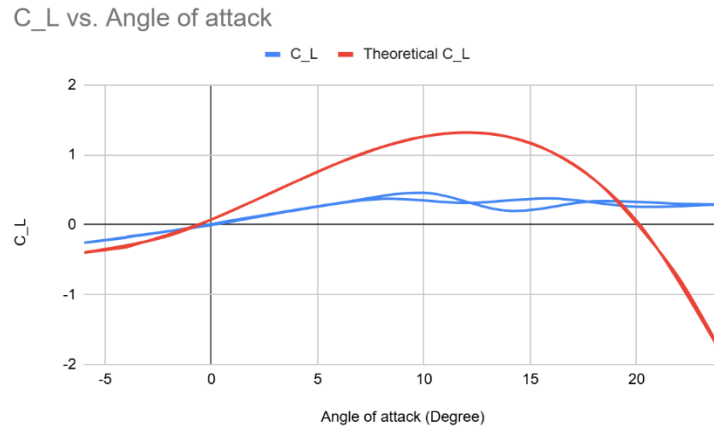


Figure 7: Comparison of Experimental and Theoretical Lift Coefficient ( $C_L$ ) vs. Angle of Attack ( $\alpha$ ) for the Clark Y-14 Airfoil

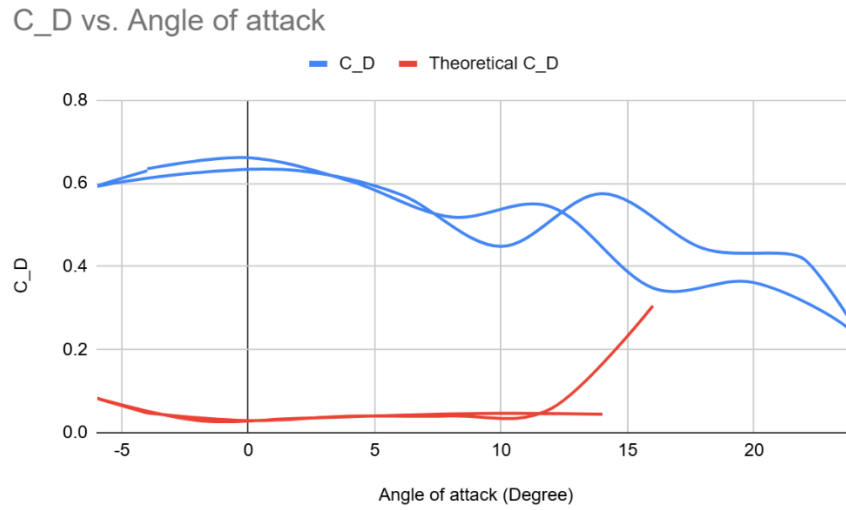


Figure 8: Comparison of Experimental and Theoretical Drag Coefficient ( $C_D$ ) vs. Angle of Attack ( $\alpha$ ) for the Clark Y-14 Airfoil

C<sub>m</sub> vs. Angle of attack

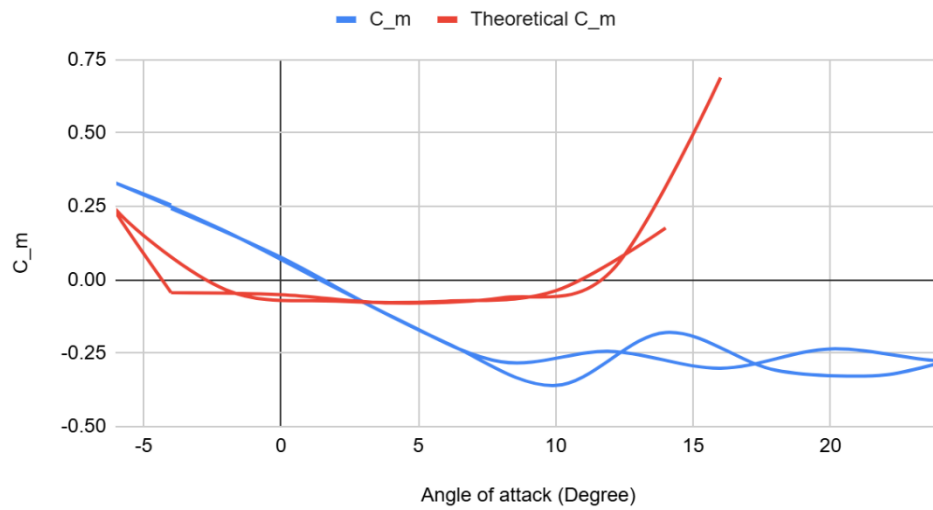


Figure 9: Comparison of Experimental and Theoretical Pitching Moment Coefficient ( $C_m$ ) vs. Angle of Attack ( $\alpha$ ) for the Clark Y-14 Airfoil

C<sub>L</sub> vs. Angle of attack

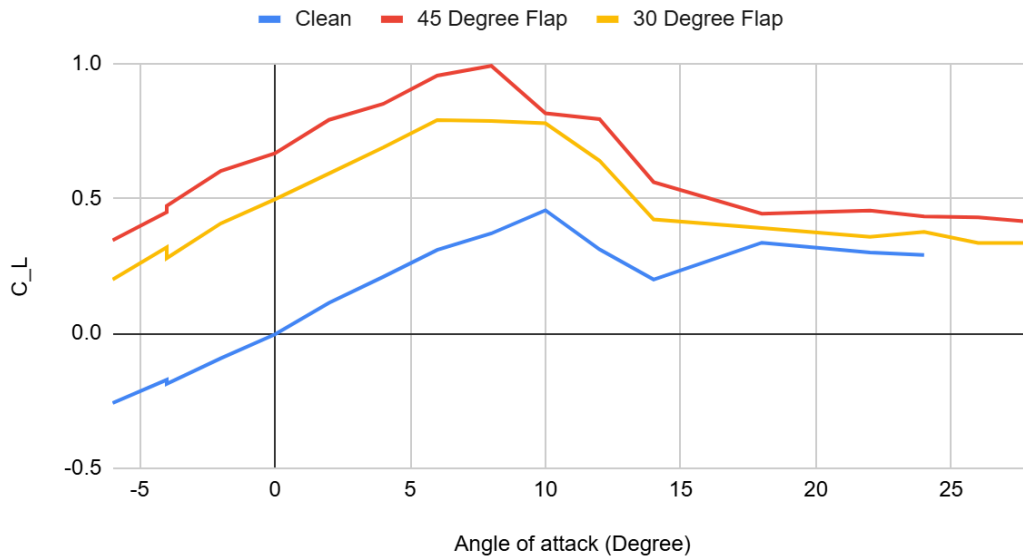


Figure 10: Lift Coefficient ( $C_L$ ) vs. Angle of Attack ( $\alpha$ ) for the Clark Y-14 Airfoil with Clean Configuration and Flaps at 30° and 45°

### C<sub>D</sub> vs. Angle of attack

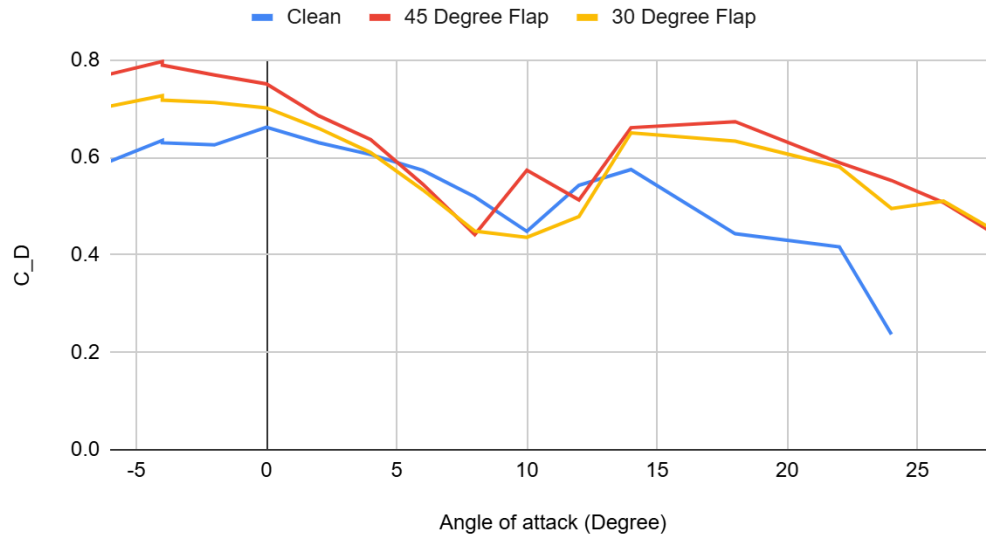


Figure 11: Drag Coefficient ( $C_D$ ) vs. Angle of Attack ( $\alpha$ ) for the Clark Y-14 Airfoil with Clean Configuration and Flaps at 30° and 45°

### L/D vs. Angle of attack

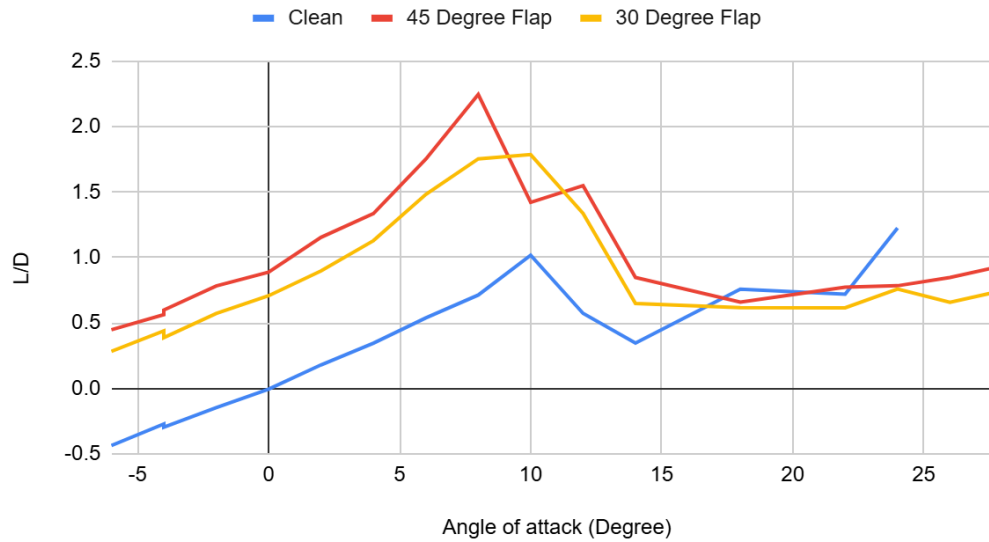


Figure 12: Lift-to-Drag Ratio ( $\frac{L}{D}$ ) vs. Angle of Attack ( $\alpha$ ) for the Clark Y-14 Airfoil with Clean Configuration and Flaps at 30° and 45°

## 7. Conclusion

The experiment successfully analyzed the aerodynamic performance of the Clark Y-14 airfoil under various configurations, including clean, slat-only, flap-only, and combined slat-flap setups. Wind tunnel testing across free-stream velocities of 10 m/s, 20 m/s, and 25 m/s revealed significant variations in the lift ( $C_L$ ), drag ( $C_D$ ), and pitching moment ( $C_M$ ) coefficients as a function of the angle of attack ( $\alpha$ ) and configuration. The results of these experiments provide key insights into the effects of slats and flaps on the aerodynamic performance of the airfoil, particularly with respect to the lift-to-drag ratio and stall characteristics.

In conclusion, the results of this experiment underscore the importance of slats and flaps in improving the aerodynamic performance of airfoils, particularly in terms of enhancing lift and delaying stall. These modifications not only improve the lift-to-drag ratio in high-lift scenarios but also provide better stability near the stall condition. The application of wall corrections further ensured the accuracy of the results, aligning them with expected real-world behavior. The findings have significant implications for airfoil design, particularly in optimizing performance for different flight phases. Future research could focus on refining these designs and exploring additional modifications to improve aerodynamic efficiency and safety.

## 8. Acknowledgments

We want to thank Professor Sherif Hassaan for his guidance and instruction, which provided a solid theoretical foundation for understanding the purpose and scope of this experiment. We would also like to thank Teaching Assistant Cody Gonzalez for his assistance during the experiment, helping ensure that the procedures were conducted smoothly and accurately.

## 9. References

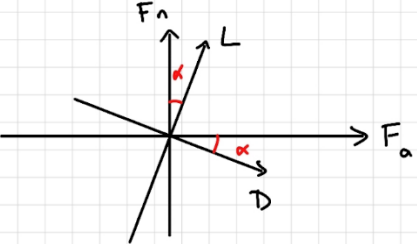
- [1] MAE 108 Laboratory Manual
- [2] Sherman, Albert. *Airfoil Section Characteristics as Affected by Variations of the Reynolds Number* [Online]. Retrieved from: <https://ntrs.nasa.gov/citations/19930091662> (Accessed: 19 November 2024).

## **10. Appendices**

### **Appendix 1: Sample computations**

This section will include sample computations that were done to reduce the data down to the final results.

Calculation for lift and drag force



$$L = F_n \cos \alpha - F_a \sin \alpha$$

$$D = F_a \cos \alpha + F_n \sin \alpha$$

Calculation for lift and drag coefficient

$$C_L = \frac{L}{\frac{1}{2} \rho V^2 S_{REF}}$$

$$C_D = \frac{D}{\frac{1}{2} \rho V^2 S_{REF}}$$

Calculation for pitching moment

$$M = \frac{T_y}{(0.175 \times 0.0565) \times 25^2 \times 1.208}$$

Calculation for pitching moment  $C_m$

$$C_m = \frac{M}{\frac{1}{2} \rho V^2 S_{REF}}$$

Calculation for pitching moment coefficient  $C_{m,ac}$

$$C_{m,ac} = C_m - C_L \left( \frac{x_{ac}}{c} \right)$$

## **Appendix 2: Experimental data**

The following chart shows recorded data from the experiment.



**Table 1: Clean airfoil with velocity at 0 m/s**

$\alpha$ (degree)	Fx (N)	Fz (N)	Ty (Nmm)
-8	-1.46804	-2.57659	-91.1594
-6	-1.47312	-2.63442	-91.3967
-4	-1.48053	-2.69745	-91.5351
-2	-1.48216	-2.77846	-91.6366
0	-1.47701	-2.88202	-91.6616
2	-1.47442	-2.93373	-91.506
4	-1.47234	-2.99059	-91.2036
6	-1.46904	-3.04139	-90.871
8	-1.45681	-3.09796	-90.5866
10	-1.44723	-3.13129	-90.0801
12	-1.43406	-3.18543	-89.5263
14	-1.42372	-3.21783	-88.9251
16	-1.40456	-3.2635	-88.2772
18	-1.39081	-3.25604	-87.5828
20	-1.37318	-3.24901	-86.6501
22	-1.351	-3.26621	-85.7502
24	-1.32738	-3.31875	-84.7743
26	-1.30226	-3.31109	-83.6122
28	-1.27675	-3.36873	-82.7135
30	-1.27675	-3.36873	-82.7135

**Table 2: Clean airfoil with velocity at 10 m/s**

$\alpha$ (degree)	Fx (N)	Fz (N)	Ty (Nmm)
-4	-1.50215	-2.721	-96.1105
0	-1.24941	-2.83677	-82.7844
4	-1.03316	-2.9509	-70.8318
8	-0.906185	-3.07232	-64.7818
12	-0.833507	-3.18971	-61.6769
16	-0.711772	-3.29999	-55.975
20	-0.580752	-3.40131	-49.893
24	-0.442359	-3.56405	-44.9318
28	-0.319565	-3.52057	-39.4731
32	-0.162195	-3.57429	-32.5535
30	-0.239627	-3.60924	-35.8899
26	-0.373019	-3.53526	-41.6545
22	-0.520162	-3.41617	-47.9484
18	-0.645856	-3.3914	-53.6177
14	-0.767346	-3.2807	-59.1793
10	-0.874629	-3.15153	-64.3694
6	-1.01604	-3.02338	-71.2516
2	-1.12776	-2.92275	-77.1463
-2	-1.35343	-2.81749	-89.7226
-6	-1.62186	-2.70257	-103.791
-4	-1.47585	-2.78738	-95.7928

**Table 3: Clean airfoil with velocity at 20 m/s**

$\alpha$ (degree)	Fx (N)	Fz (N)	Ty (Nmm)
-4	-0.962373	-2.87322	-79.9941
0	-0.0178273	-2.91808	-25.0849
4	1.11691	-2.75606	40.4703
8	2.01314	-2.59446	91.7795
12	2.01404	-2.87537	80.2328
16	2.38054	-2.27961	99.1858
20	2.09885	-2.45926	77.4581
24	2.37995	-2.20247	90.5701
22	2.66004	-3.05567	106.652
18	2.48684	-2.86314	101.261
14	1.6603	-3.02781	59.0278
10	2.47189	-2.44304	118.466
6	1.65615	-2.71738	70.4329
2	0.597499	-2.8017	9.39616
-2	-0.504352	-2.77841	-54.1528
-6	-1.43755	-2.7767	-108.147
-4	-1.02606	-2.85665	-83.9604

**Table 4: Clean airfoil with velocity at 25 m/s**

$\alpha$ (degree)	Fx (N)	Fz (N)	Ty (Nmm)
-4	-0.730619	-2.7895	-76.4454
0	0.872336	0.872336	17.0829
4	2.76487	-2.63626	125.472
8	4.10705	-2.29676	201.99
12	4.98186	-1.8889	252.584
16	5.09122	-2.38128	-81.0169
20	4.78878	-2.91517	212.478
24	4.97019	-3.316	213.275
22	5.20539	-3.20051	227.288
18	4.7285	-2.89337	208.444
14	4.62891	-2.48196	216.277
10	4.86196	-2.08783	244.275
6	3.65049	-2.51249	172.769
2	1.86597	-2.84499	70.9783
-2	0.0741441	-2.9109	-32.045
-6	-1.28805	-2.83289	-110.697
-4	-0.633635	-2.92001	-72.9027

**Table 5: Airfoil with Slat and 5 mm separation, velocity at 0 m/s**

$\alpha$ (degree)	F <sub>x</sub> (N)	F <sub>z</sub> (N)	T <sub>y</sub> (Nmm)
-6	-1.53204	-2.46434	-111.558
-4	-1.54152	-2.54024	-111.958
-2	-1.54152	-2.54024	-111.958
0	-1.55178	-2.74353	-112.338
2	-1.55283	-2.79804	-112.292
4	-1.55283	-2.79804	-112.292
6	-1.54933	-2.92925	-112.026
8	-1.54501	-2.99446	-111.777
10	-1.54081	-3.04591	-111.53
12	-1.52879	-3.12878	-110.985
14	-1.51984	-3.18707	-110.467
16	-1.49886	-3.28359	-109.469
18	-1.48826	-3.32747	-108.926
20	-1.47025	-3.38611	-108.023
22	-1.44447	-3.4612	-106.783
24	-1.42842	-3.50872	-106.032
26	-1.40265	-3.55843	-104.817
28	-1.37113	-3.60895	-103.304
30	-1.33683	-3.65394	-101.569

**Table 6: Airfoil with Slat and 5 mm separation, velocity at 20 m/s**

$\alpha$ (degree)	Fx (N)	Fz (N)	Ty (Nmm)
-6	-2.24989	-3.02004	-170.91
-4	-1.84233	-3.04342	-151.131
-4	-1.8347	-3.02904	-151.711
-2	-1.46241	-2.98603	-132.654
0	-1.06437	-2.99805	-108.992
2	-0.682502	-2.92195	-85.3195
4	-0.463488	-2.99587	-68.8738
6	0.0779143	-2.98085	-35.7804
8	0.274663	-2.69093	-23.1806
10	1.06206	-2.88091	20.7798
12	1.51502	-2.54981	47.0388
14	1.78335	-2.69205	60.6019
16	2.01602	-2.6145	75.2803
18	1.80815	-2.96984	50.0282
20	2.1132	-2.48862	74.8683
22	1.71914	-3.34945	44.0058
24	1.75633	-3.00014	46.7877
26	1.99119	-3.38328	62.7636
28	2.30758	-2.83672	82.8306

**Table 7: Airfoil with Slat/Flap, 45° Flap, 5 mm separation, and velocity at 0 m/s**

$\alpha$ (degree)	F <sub>x</sub> (N)	F <sub>z</sub> (N)	T <sub>y</sub> (Nmm)
-6	-1.85333	-2.33826	-121.584
-4	-1.8648	-2.4208	-122.079
-2	-1.87203	-2.4955	-122.415
0	-1.8784	-2.58105	-122.704
2	-1.88099	-2.69604	-122.868
4	-1.87983	-2.76849	-122.869
6	-1.87353	-2.87568	-122.756
8	-1.86832	-2.95085	-122.581
10	-1.85409	-3.07174	-122.061
12	-1.84213	-3.14602	-121.622
14	-1.82638	-3.22156	-121.082
16	-1.80401	-3.31236	-120.302
18	-1.7835	-3.38721	-119.588
20	-1.75456	-3.4793	-118.452
22	-1.73582	-3.52834	-118.004
24	-1.70401	-3.6135	-116.817
26	-1.67693	-3.66215	-115.791
28	-1.63648	-3.72958	-114.2
30	-1.51063	-3.87347	-109.318

**Table 8: Airfoil with Slat/Flap, 45° Flap, 5 mm separation, and velocity at 20 m/s**

$\alpha$ (degree)	F <sub>x</sub> (N)	F <sub>z</sub> (N)	T <sub>y</sub> (Nmm)
-6	0.883411	-3.43038	-29.37
-4	1.6245	-3.52825	16.5368
-4	1.64725	-3.51837	
-2	2.07987	-3.50191	37.9491
0	2.5557	-3.4994	68.9005
2	3.17306	-3.37246	101.004
4	3.605	-3.17829	128.31
6	4.25005	-3.11625	164.037
8	4.49897	-2.84689	184.69
10	4.04386	-3.48945	148.21
12	4.66397	-2.61366	201.343
14	4.23346	-3.59009	164.416
16	4.4865	-3.1121	181.31
18	3.62684	-4.27245	121.556
20	4.36886	-2.90119	171.403
22	4.25956	-4.05128	161.226
24	4.41872	-3.76596	172.163
26	4.65465	-4.06512	181.737
28	4.89154	-3.92396	194.273



**Table 9: Airfoil with Flap, 45° Flap, and velocity at 0 m/s**

$\alpha$ (degree)	Fx (N)	Fz (N)	Ty (Nmm)
-6	-1.64689	-2.49962	-102.685
-4	-1.65254	-2.57538	-102.988
-2	-1.65654	-2.64864	-103.119
0	-1.65613	-2.7182	-103.181
2	-1.6526	-2.79074	-103.154
4	-1.64755	-2.88186	-103.014
6	-1.64293	-2.92247	-102.88
8	-1.63264	-3.00368	-102.592
10	-1.61876	-3.09232	-102.12
12	-1.6008	-3.17139	-101.596
14	-1.58259	-3.2449	-100.963
16	-1.5669	-3.30332	-100.427
18	-1.54431	-3.37065	-99.7196
20	-1.52083	-3.43824	-98.8927
22	-1.49183	-3.4999	-97.9233
24	-1.46919	-3.54242	-97.1633
26	-1.42532	-3.61652	-95.6067
28	-1.39379	-3.664	-94.5484
30	-1.36959	-3.70131	-93.7024

**Table 10: Airfoil with Flap, 45° Flap, and velocity at 20 m/s**

$\alpha$ (degree)	F <sub>x</sub> (N)	F <sub>z</sub> (N)	T <sub>y</sub> (Nmm)
-6	1.18398	-3.29439	2.91821
-4	1.74527	-3.40011	35.2529
-4	1.85231	-3.35919	38.7752
-2	2.54012	-3.30588	76.654
0	2.94156	-3.31119	101.659
2	3.60073	-3.15085	137.168
4	3.97403	-3.09207	159.288
6	4.53842	-2.89503	189.687
8	4.78491	-2.63886	205.21
10	4.23622	-3.31637	165.924
12	4.26246	-3.21744	167.49
14	3.51383	-3.8803	119.966
16	3.44171	-3.718	114.441
18	3.4327	-4.23787	113.585
20	3.62571	-4.20584	119.741
22	3.94027	-4.3947	135.476
24	4.09076	-4.48944	138.252
26	4.35989	-4.61502	149.159
28	4.50921	-4.60248	155.054

**Table 11: Airfoil with Flap, 30° Flap, and velocity at 0 m/s**

$\alpha$ (degree)	Fx (N)	Fz (N)	Ty (Nmm)
-6	-1.63683	-2.42673	-103.455
-4	-1.64295	-2.51988	-103.778
-2	-1.6477	-2.61088	-103.941
0	-1.64677	-2.66846	-103.983
2	-1.64512	-2.74246	-103.966
4	-1.64008	-2.80976	-103.88
6	-1.6293	-2.92139	-103.549
8	-1.61981	-2.9892	-103.295
10	-1.60657	-3.0626	-102.861
12	-1.58977	-3.13623	-102.354
14	-1.57391	-3.19789	-101.821
16	-1.55008	-3.2798	-101.014
18	-1.52893	-3.33995	-100.323
20	-1.50295	-3.40957	-99.4653
22	-1.47603	-3.4704	-98.4992
24	-1.45198	-3.51898	-97.7144
26	-1.42862	-3.56133	-96.8508
28	-1.38336	-3.63701	-95.2663
30	-1.34168	-3.69061	-93.8031

**Table 12: Airfoil with Flap, 30° Flap, and velocity at 20 m/s**

$\alpha$ (degree)	Fx (N)	Fz (N)	Ty (Nmm)
-6	0.560925	-3.06828	-22.0458
-4	1.19066	-3.12893	15.6069
-4	1.01388	-3.10054	4.32111
-2	1.68986	-3.0849	41.1564
0	2.18944	-3.09389	71.4356
2	2.71765	-3.00624	98.9632
4	3.24706	-2.9233	130.257
6	3.79403	-2.76389	159.522
8	3.85933	-2.54022	166.855
10	3.95276	-2.64905	173.238
12	3.50126	-2.90237	139.091
14	2.83144	-3.66194	97.3411
16	2.81165	2.81165	94.5892
18	3.08879	-3.93996	106.067
20	2.95458	2.95458	97.6252
22	3.36515	-4.12115	116.625
24	3.59007	-3.98853	124.949
26	3.75969	-4.33732	129.893
28	3.99205	-4.36291	139.56